Increased RhoA pathway activation downstream of αIIbβ3/SRC contributes to heterozygous Bernard Soulier syndrome

Larissa Lordier,[1-4*] Christian A. Di Buduo,[5*] Alexandre Kauskot,[6] Nathalie Balayn,[2-4] Cécile Lavenu-Bombled,[7] Francesco Baschieri,[8] Valérie Proulle,[9,10] Cecilia P. Marin Oyarzun,[2-4] Francesca Careddu,[5] Ida Biunno,[11] Tudor Manoliu,[4,12] Philippe Rameau,[4,12] Isabelle Plo,[2-4] Nicolas Papadopoulos,[13,14] Stefan Constantinescu,[13-16] William Vainchenker,[2-4] Guillaume Nam Nguyen,[17] Paola Ballerini,[17] Remi Favier,[17] Alessandra Balduini[5,18] and Hana Raslova[2-4]

[1]INOVARION, Paris, France; [2]INSERM UMR1287, Gustave Roussy, Equipe labellisée Ligue Nationale Contre le Cancer, Villejuif, France; [3]Université Paris-Saclay, UMR 1287, Gustave Roussy, Villejuif, France; [4]Gustave Roussy, UMR 1287, Villejuif, France; [5]Department of Molecular Medicine, University of Pavia, Pavia, Italy; [6]INSERM U1176, Hemostasis, Inflammation and Thrombosis (HITh), Université Paris-Saclay, Le Kremlin-Bicêtre, France; [7]Paris Saclay University, INSERM U1176 (HITh), AP-HP, Hematology Department, Bicêtre Hospital, Le Kremlin-Bicêtre, France; [8]Institute of Pathophysiology, Biocenter, Medical University of Innsbruck, Innsbruck, Austria; [9]Service Hématologie Biologique, Hôpital Cochin, AP-HP Centre - Université Paris Cité, France; [10]Unite INSERM UMRS 1138, CRC, Paris, France; [11]Integrated Systems Engineering, Bresso-Milano, Italy; [12]UMS AMMICa 23/3655, Plateforme Imagerie et Cytométrie, Gustave Roussy, Université Paris-Saclay, Villejuif, France; [13]Ludwig Institute for Cancer Research, Brussels, Belgium; [14]Université Catholique de Louvain and de Duve Institute, SIGN Unit, Brussels, Belgium; [15]Walloon Excellence in Life Sciences and Biotechnology, Brussels, Belgium; [16]Ludwig Institute for Cancer Research, Nuffield Department of Medicine, Oxford University, Oxford, UK; [17]Assistance Publique-Hôpitaux de Paris, Hôpital Armand Trousseau, Centre de Référence des Pathologies Plaquettaires, Paris, France and [18]Department of Biomedical Engineering, Tufts University, Medford, MA, USA

**LL and CADB contributed equally as first authors.*

Correspondence: H. Raslova
Hana.Raslova@gustaveroussy.fr

Received: August 9, 2024.
Accepted: February 28, 2025.
Early view: March 6, 2025.

https://doi.org/10.3324/haematol.2024.286424

SUPPLEMENTAL FILE

MATERIAL AND METHODS

Bernard-Soulier syndrome patients

Five unrelated individuals (P1-P5) were identified with macrothrombocytopenia during routine blood tests. Upon further investigation, they were diagnosed with monoallelic (P1, P2, P3) or biallelic BSS (P4, P5). The diagnosis was confirmed through the identification of decreased ristocetin-induced aggregation and significant reductions in the platelet GPIb-V-IX complex (Cytoquant assay from Biocytex, Marseille, France) and by NGS. Platelet aggregation in response to 5-10 µM ADP, 5 µM epinephrine, 1-2.5 µg/mL collagen, 0.8-1 mM arachidonic acid, 10-25 µM TRAP and 1.5mg/L of ristocetin was performed as previously described[1] and expressed as maximal light transmission percentage (**ST1**). $CD34^+$ cells were isolated by a positive selection using an immunomagnetic cell sorting system (AutoMacs; Miltenyi Biotec, Bergisch Gladbach, Germany) and were cultured in serum-free medium containing TPO (10 ng/mL), SCF (25 ng/mL). For ploidy analysis, Hoechst 33342 (10 µg/mL; Sigma) was added in the medium at day 10 of culture for 2 h at 37C. Cells were then stained with directly coupled MoAbs: anti-CD41 APC and anti-CD42 PE (BD Biosciences) for 30 min at 4C. Ploidy was measured in the $CD41^+/CD42^+$ cell population by Fortessa (Becton Dickinson). The mean ploidy of human megakaryocytes (MKs) was calculated by the following formula: (2N x the number of cells at 2N ploidy level + 4N x the number of cells at 4N ploidy level+…+64N x the number of cells at 64N ploidy level /the total number of cells). For the analysis of proplatelet formation or platelet production, the $CD41^+CD42^+$ cells were sorted (FacsDIVA, Becton Dickinson, le Pont de Claix, France) on day 10 of culture and processed as described below.

iPSCs generation and expansion

$CD34^+$ cells were obtained from peripheral blood of P1 patient through positive selection using an immunomagnetic bead cell-sorting system (AutoMacs; Miltenyi Biotec). Subsequently, these cells were cultured in a serum-free medium that included EPO (1 U/mL), FLT3- L (10 ng/mL), G-CSF (20 ng/mL), IL-3 (10 ng/mL), IL-6 (10 ng/mL), SCF (25 ng/mL), TPO (10 ng/mL), and GM-CSF (10 ng/mL) for 6 days. Following this expansion phase, the cells underwent transduction using the CytoTune iPS 2.0 Sendai Reprogramming Kit (Thermo Fisher), and the reprogramming process was carried out according to the manufacturer's instructions. Colonies exhibiting an embryonic stem (ES)-like morphology were manually isolated, expanded for a reduced number of passages, and then cryopreserved. The induced

pluripotent stem cells (iPSCs) were cultured in StemMACS iPS-Brew medium (Miltenyi Biotech) on plates coated with N-truncated Human recombinant Vitronectin (Gibco). Regular cell passages were carried out using a 500 mM EDTA solution in 1X PBS. Routine Mycoplasma screening, following the manufacturer's instructions (Sigma), was performed. To minimize the risk of karyotypic and genomic anomalies, cells were maintained for a limited number of passages in culture.

qRT-PCR analysis of pluripotency markers

The validation of self-renewal stem cell markers (*SOX2*, *OCT4* and *NANOG*) was conducted through qRT-PCR analysis. The DDCt method was employed on the Rotor-Gene Q system (Qiagen) using the Maxima SYBR Green qPCR Master Mix (ThermoFisher Scientific). GAPDH was chosen as the housekeeping gene, and the data were normalized to its expression. Statistical analysis was carried out using the REST (Relative Expression Software Tool) software. The expression of self-renewal stem cell markers in GPIbα^{N103D} clones was compared to that in hESCs RC17 (Rosalin Cells, Edinburgh, UK) and hiPSCs CTR2#6.

Karyotype Analysis

On the 4th day post-split, induced pluripotent stem cells (iPS-cells) underwent a 3-hour treatment with 0.1 μg/mL Colcemid. A total of 32 to 38 metaphases were examined, and among them, 13-15 metaphases were karyotyped using QFQ-banding. The q-Bands were visualized through Fluorescence using Quinacrine and observed with a Fluorescence Microscope Olympus CHB (BX63) equipped with a quinacrine mustard filter and CCD camera. The analysis was performed using Bright-Field Microscope "GenASIs" Software, version 8.1.0.47741, developed by Applied Spectral Imaging.

Short Tandem Repeat (STR) Testing Report

Polymerase chain reaction (PCR) was employed to amplify nine autosomal short tandem repeat (STR) molecular markers (D21S11, D7S820, CSF1PO, TH01, D13S317, D16S539, vWA, TPOX, D5S818) along with the gender-determining marker Amelogenin, utilizing the Promega GenePrint 10 Kit as per the manufacturer's recommended protocol. Positive and negative amplification controls were included following the kit's guidelines. The resulting amplified products were subjected to analysis on an ABI Prism® 3730xl Genetic Analyzer, utilizing an

Internal Lane Standard 600 (Promega). Data generated were then analyzed using GeneMapper® Software version 4.0 (Applied Biosystems) in accordance with the manufacturer's instructions.

iPSCs hematopoietic differentiation

Clusters of pluripotent cells were seeded on Geltrex (Gibco)-coated plates in the presence of IPS-Brew medium at day -1. The initial cell concentration was adjusted for each cell line to achieve a 10-20% confluency range. On Day 0, cells were transferred to a xeno-free medium based on StemPro-34 SFM (Gibco), supplemented with 1% v/v Penicillin/Streptomycin (Gibco), 1% v/v L-Glutamine (Gibco), 0.04 mg/mL 1-Thioglycerol (Sigma), and 50 µg/mL ascorbic acid (Sigma). This medium was maintained throughout the experiment and supplemented with various cytokines and growth factors according to the following schedule:

- Days 0 – 2: BMP4 (10 ng/mL), VEGF (50 ng/mL), and CHIR99021 (2 µM).
- Days 2 – 4: BMP4 (10 ng/mL), VEGF (50 ng/mL), and bFGF (20 ng/mL).
- Days 4 – 6: VEGF (15 ng/mL) and bFGF (5 ng/mL).
- Day 6: VEGF (50 ng/mL), bFGF (50 ng/mL), SCF (25 ng/mL), and FLT3L (5 ng/mL).
- Days 7-10: VEGF (50 ng/mL), bFGF (50 ng/mL), SCF (25 ng/mL), FLT3L (5 ng/mL), TPO (25 ng/mL), and IL-6 (10 ng/mL).
- Days 10-20: SCF (25 ng/mL) and TPO (25 ng/mL).

Manufacturers of the components are detailed in Supplemental Table 2 (**ST2**).

Flow Cytometry

Single cell suspensions were subjected to staining using monoclonal antibodies directly coupled to their respective fluorochromes, as listed in **ST3**. The antibodies were applied to cells at a concentration of 1 µL per 10^6 cells in approximately 100 µL, and the incubation was carried out at 4°C for at least 30 minutes. Both before and after incubation, cells were washed with PBS 1X. Analysis was conducted using BD Canto II or BD LSRFortessa cytometers (BD Biosciences). For the isolation of MKs, Fluorescence Activated Cell Sorting (FACS) was routinely employed and executed on Influx, ARIA III, or ARIA Fusion cell sorters (BD Biosciences).

Proplatelet formation assay

Proplatelet formation was evaluated either on MKs cultured in a serum-free medium containing TPO (10 ng/mL) and SCF (25 ng/mL) or after 2-3 days adhesion on fibrinogen (20 µg/mL) by enumerating no less than 200 cells per well, utilizing an inverted microscope (Carl Zeiss) at a 200x magnification.

Immunoblot analysis

Cells: Cell lysis was carried out using 2x Laemmli buffer supplemented with a cocktail of protease inhibitors. Following lysing, proteins underwent separation by SDS-PAGE and were subsequently transferred onto nitrocellulose membranes. The membranes were blocked for 1 hour using a 5% w/v BSA solution in Tween-PBS 1X. Primary antibodies were then incubated overnight, followed by a 1-hour incubation with secondary antibodies coupled to horseradish peroxidase. Both types of antibodies were diluted in a solution of 5% w/v BSA in Tween-PBS 1X. Primary and secondary antibodies, including clone names, concentrations, and manufacturers, are listed in Supplemental table 3 (**ST3).**

Supernatant: To analyze soluble GPIbα in the culture medium, 150 000 ($CD41^+CD33^-$) MKs were sorted on day 13 of culture, seeded in 150 µl of serum-free medium containing TPO and SCF and four days later, the cells were centrifuged at 3000 rpm to remove all cells and cellular debris. 10 µl of supernatant was used for WB analysis. Recombinant soluble GPIbα $(rGPIb)^2$ was used as a control.

Band detection was performed by enhanced chemiluminescence system (ECL or SuperSignal West Pico Plus kit; Life Technologies) using Image Quant LAS 4000 (GE Healthcare)/iBright FL1500 (Thermo Fisher Scientific). The quantification was by ImageJ2 software.

Immunoprecipitation assay

iPSC were lysed with lysis buffer containing 1% Triton X-100, 150 mM NaCl, 50 mM Tris pH 7.4, 5 mM EGTA, 1 mM Na_3VO_4, 1x Halt Protease Inhibitor Cocktail. GPIbα was precipitated by incubation of the lysates with an anti-GPIbα antibody (clone SZ2, 2 µg)-coated protein G-magnetic beads 1h at RT. Supernatant was collected and the magnetic beads were washed 3 times with 1x lysis buffer before 2x Laemmli buffer was added. Samples were separated by SDS–PAGE.

Proteome Phospho-Kinase Array

The impact of a fibrinogen binding to αIIbβ3 on the phosphorylation of kinases in MKs was investigated using a membrane-based human phospho-kinase antibody array kit (ARY003B, R&D Systems, Minneapolis, MN, USA), designed to profile 46 specific phosphorylation sites. According to the manufacturer's instructions, mature MKs were plated on a fibrinogen-coated surface for 30 minutes at 37°C. Subsequently, the corresponding cell lysates were incubated with the pre-blocked membrane overnight at 4 °C. On the following day, the membrane underwent extensive rinsing and was then incubated with biotinylated detection antibodies (antibody cocktail) at room temperature for 2 hours. Following this, the membrane was exposed to a diluted streptavidin-horseradish peroxidase (HRP) solution at room temperature for 30 minutes, and visualization was achieved using a chemi-reagent mix. Detection and quantification of pixel density for the obtained spots were performed using Image Quant LAS 4000 (GE Healthcare) and ImageJ software Version 1.51n, respectively. The results were expressed as the relative phosphorylation level of the corresponding kinase.

Von Willebrand Factor binding assays

Purified MKs underwent incubation with human von Willebrand Factor (VWF) at concentrations ranging from 0 to 0.5 μg/mL in the presence of the VWF-modulator ristocetin (0.5 mg/mL) for 15 minutes at room temperature. Following this, cells were fixed with 1% paraformaldehyde for 5 minutes. Washed cells were then treated for 30 minutes with an anti–human VWF-specific monoclonal antibody (mAb) and subsequently with Alexa Fluor 488–anti-Rabbit Antibody. Flow cytometry was employed for analysis. To block VWF binding to human GPIbα, the anti–human GPIbα-specific monoclonal antibody SZ2 (0.5 or 1μg) was utilized. MKs were preincubated for 15 minutes with the anti–human GPIbα blocking antibody before incubation with human VWF, following the previously described treatment. The antibodies used are listed in Supplemental Table 2 (**ST3**).

aIIbβ3 activation assay

The activation of integrin αIIbβ3 was assessed through flow cytometry. MKs were suspended in Tyrode's buffer, incubated with either Alexa Fluor 647-labeled PAC1 antibody or Alexa 488-labeled Fibrinogen, in the presence or absence of thrombin (1U/mL) for 5 minutes at 37°C. Following this, cells were fixed with 1% paraformaldehyde and analyzed on a BD Canto II flow

cytometer (BD Biosciences, Franklin Lakes, NJ, USA). The antibodies used are listed in Supplemental Table 3 (**ST3**).

Immunofluorescence microscopy and fluorescence quantification

Mature MKs were plated on poly L-lysine-coated slides, for 1 hour at 37°C, or cultured in adhesion onto fibrinogen, as described above. Subsequently, they were fixed with 4% paraformaldehyde, permeabilized using 0.1% Triton X-100, and stained with anti-β-tubulin, anti-P-MLC2, anti-FLNa, anti-CD42b, or anti-VWF antibodies. This was followed by incubation with secondary Alexa Fluor-488 goat anti-mouse or anti-rabbit antibodies, Alexa Fluor 555–phalloidin or Alexa Fluor 488-phalloidin or Alexa Fluor 633-phalloidin and DAPI for visualization of specific cellular components. A detailed list including the concentration, clone name, and manufacturer for each antibody can be found in Supplemental Table 3 (**ST2**).

Coverslips were mounted in Mowiol for observation under a confocal microscope Leica SP8 (Danaher Corporation, objective 63XNA1.40) using LAS acquisition software (AF version 1.62; Leica). Image analysis was subsequently performed with the LASX software. To quantify the distribution of fluorescent signal between different experimental conditions and to measure the area of pro-platelet tips, confocal microscopy images were analyzed using Fiji software (ImageJ 2.1.0). The analysis workflow involved several steps: 1) Image Preprocessing: Confocal images were opened in Fiji (.lif format), the "Split Channels" function was used to separate the four fluorescence channels. For each channel, a Z-stack projection was created using the "SUM" method to generate a single image representing the total intensity across the Z-stack. 2) Region of Interest (ROI) Definition: *Membrane ROI:* Four rectangular ROI were defined for each image and placed at the edge of the cell, including the membrane and slightly encompassing the cytoplasm. *Nuclear-Excluding Cytoplasmic ROI:* A square ROI placed at the center of the cell, avoiding the nucleus region. *Tip ROI:* For pro-platelet tip area measurement, a separate ROI was created encompassing the tip of the pro-platelet. 3) Thresholding: An automatic Otsu thresholding method[3] was applied to each ROI to separate the fluorescent signal from the background. This method dynamically sets the threshold based on the image histogram, ensuring optimal signal segmentation. 4) Fluorescence Intensity Measurement: The mean fluorescence intensity was measured for each ROI and fluorescence channel. This provided quantitative data on the distribution of fluorescent signal within the membrane/cytoplasm and nuclear-excluding region. 5) Pro-Platelet Tip Area Measurement: The area of the pro-platelet tip ROI was measured in microns squared. 6) Data Analysis: The

data was collected from at least 11 cells per experimental condition (4 conditions in total, 2 different controls and 2 different GPIbα^{N103D} clones). The ratio between the mean intensity in the membrane ROI and the nuclear-excluding cytoplasmic ROI was calculated for each cell and condition. This ratio provided a measure of the relative distribution of fluorescent signal within the cell. For the analysis of proplatelet tips, the area of tips was analyzed and fluorescence measurements were calculated per 1μm^2 and compared between different conditions.

MK spreading and stress fiber formation

Slides were coated with human VWF (1 μg/mL) and ristocetin (0.5 mg/mL), fibrinogen (20 μg/mL), or fibronectin (25 μg/mL) in PBS buffer overnight at 4°C. They were subsequently blocked with BSA (5 mg/mL) for 1 hour at room temperature and washed with PBS before use. Mature MKs were then plated on surfaces coated with fibronectin, fibrinogen, or VWF for 30 minutes at 37°C. In experiments involving dasatinib, mature MKs were incubated for 15 minutes with dasatinib (10 μM) and then plated on a fibrinogen-coated surface for 30 minutes at 37°C. For experiments involving the ROCK1/2 inhibitor, MKs were plated with or without Y27632 (10 μM) on a fibrinogen-coated surface for 30 minutes at 37°C. In experiments with thrombin, thrombin (1U/mL) was added to the cell suspension and immediately after, MKs have adhered on fibrinogen. Adhered MKs were fixed with 4% paraformaldehyde, permeabilized using 0.1% Triton X-100, and stained with Alexa Fluor 488–phalloidin and DAPI. A detailed list containing the concentration, clone name, and manufacturer for each antibody can be found in Supplemental Table 2 (**ST2**). The adhesion and spreading of MKs were visualized using differential interference contrast (DIC) microscopy (DMIRB, 63× or 100× Objective; Leica), and images were captured using DVT tools (Pinnacle Systems). Image analysis was subsequently performed with the LASX software. Quantification of the number of adherent and spreading MKs was conducted by analyzing at least three random fields.

Preparation of silk fibroin scaffolds

Silk fibroin aqueous solution was obtained from *B. mori* silkworm cocoons according to previously published literature.[3] Briefly, fibroin was obtained by boiling cocoons in Na_2CO_3. The fibers were rinsed in ultrapure water and dried at room temperature (RT) for 48 h. The dried fibers were subsequently solubilized in Lithium Bromide solution for 4 h at 60 °C. The silk solution was then dialyzed against deionized water using a Slide-A-Lyzer cassette (Thermo

Fisher). Silk scaffolds have been produced by a salt-leaching method and functionalized with 50 µg/mL fibrinogen or 50 µg/mL fibronectin, as previously described.[4-7]

Silk bone marrow assembly and perfusion

The dynamic perfusion of the silk bone marrow scaffold was performed by using a peristaltic pump (ShenChen Flow Rates Peristaltic Pump - LabV1) connected to a bioreactor chamber manufactured using 3D SLA printing technology (Form 3B (Formlab)). The chamber was designed using CAD software (Fusion 360). The printing was performed using the Biomed Clear biocompatible resin cured in layers of 100 µm. The resulting chamber was washed with isopropyl alcohol (IPA) to remove the unpolymerized resin and then cured in a UV oven for 1 h. The resulting flow chamber consisted of two wells of 10 (L) × 5 (W) × 5 (H) mm having independent inlets and outlet channels. Each well was equipped with a silk fibroin scaffold. 1.5×10^5 MKs were seeded into each silk scaffold and kept at 37 °C and 5% CO_2. Scaffolds have been sterilized and rinsed in the culture medium before cell seeding.

Flow cytometry analysis of platelets

Flow cytometry settings for *ex vivo* generated platelets were established, as previously described.[5-7] Briefly, *ex vivo* collected platelets were analyzed using the same forward and side scatter pattern as human peripheral blood and identified as $CD41^+CD42a^+$ events. Isotype controls were used as a negative control to exclude non-specific background signals. The platelet number was calculated using a Tru-Count bead standard (Beckton Dickinson). Samples were acquired using a BD FACS Lyric (Becton Dickinson) or BD Canto II flow cytometer (Becton Dickinson). Off-line data analysis was performed using Kaluza software package (Beckman Coulter) or FlowJo v9.3.2 software (Becton Dickinson).

Imaging of the 3D silk bone marrow model

For immunofluorescence imaging within the silk bone marrow scaffold, samples were fixed in 4% PFA for 20 min and then blocked with 5% bovine serum albumin (BSA, Sigma) for 30 min at RT. Samples were stained with anti-CD61 (#IM0540) (1:100) (Beckman Coulter) diluted in 1% BSA, overnight at 4 °C. Then, samples were immersed in Alexa Fluor secondary antibody (1:200) diluted in 1% BSA for 2 hours at RT. Nuclei were stained with Hoechst. Silk fibroin fluorescence was brightened by Hoechst.[7] 3D reconstructions and image processing were performed using Leica LasX (Leica) and Arivis Vision 4D (Zeiss). Platelet diameters were

measured by Arivis Vision 4D (Zeiss). The analyses of samples have been performed blinded to genotype.

Transmission electron microscopy

MKs were fixed in 2% glutaraldehyde in 0.1M phosphate buffer for 1 hour at 4°C and postfixed with 2% osmium tetroxide in 0.1M phosphate buffer for 1 hour at room temperature. After dehydration through a graded ethanol series, samples were embedded in Epon™ 812, and polymerization was completed after 48 hours at 60 °C. Ultrathin sections were stained with standard uranyl acetate and lead citrate and observed with a FEI Tecnai 12 electron microscope. Digital images were captured using a SIS MegaviewIII CCD camera.

FRET analysis

The lentiviral RhoA or Cdc42 FRET sensors (pPBbsr2-Raichu-2707x, pRaichuEV-Cdc42-KRasCT pCSIIbsr-2280x) were generously provided by Dr. Matsuda. Viral particles were produced following the procedure as previously described.[8] MKs derived from induced pluripotent stem (iPS) cells were transduced, and cells expressing CFP and YPet were selected through FACS. Subsequently, the transduced MKs were plated on a fibrinogen-coated surface for 30 minutes at 37 °C. Slides were mounted with Fluoromount-G® (Southern Biotech).

Förster resonance energy transfer (FRET) was performed on a confocal microscope Leica SP8 with a 63X objective (1.4 NA) using the acceptor photo-bleaching method through the FRET-AB wizard of the Leica software. Briefly, the acceptor fluorophore (YPet) fluorescence was bleached at 100% laser intensity, with a minimal extent of bleaching set at 75%. This resulted in an increased fluorescence intensity of the donor fluorophore (CFP) in the bleached region, which was subsequently measured. FRET efficiency was obtained using the formula:

$$FRET_{eff.} = \frac{CFP_{post} - CFP_{pre}}{CFP_{post}}$$

Statistics

All data are shown as mean ± SEM, mean±SD or as mean ± min to max. The statistical analyses were performed using the PRISM software. Statistical significance was established using a Student's *t* test or a One Way Analysis of Variance (ANOVA) specified in legends. Differences were considered significant at $P < 0.05$.

Supplemental Table 1

Patient	Mutation	Sex/age	Platelet count	ISTH-BAT score	Platelet aggregation (%)					
		(years)	(x10^9/L)		ADP	EPI	COL	AA	TRAP	Ristocetin
P1	GPIbα^{N103D} (heterozygous)	F/62	118	2	80	70	80	70	80	75
P2	GPIbα^{L160P} (heterozygous)	F/40	88*	0	60	50	50	65	65	50
P3	GPIbα^{N150S} (heterozygous)	F/12	90*	7	42	ND	41	41	50	49
P4	GPIbβ^{G43W} (homozygous)	F/11	50-130*	1	55	ND	57	60	53	60
P5	GPIbα^{L139P} (homozygous)	M/28	16*	7	59	ND	64	ND	55	<10

Supplemental table 1: Patient characterization

Patient features. ISTH-BAT: International Society on Thrombosis and Hemostasis-bleeding assessment tool; ADP: adenosine diphosphate; ATP: adenosine triphosphate; EPI: epinephrin; COL: collagen; AA: arachidonic acid; TRAP: thrombin receptor activating peptide.

* PRP< 150 G/L, the results could be innacurate, ND: not done

Platelet aggregation in response to ADP, EPI, COL, AA, TRAP and ristocetin is expressed as maximal light transmission percentage.

Concentration of ADP, COL 1, AA, TRAP, Ristocetin:

P1, P2: ADP 5mM, EPI 5mM, COL 1mg/mL, AA 1mM, TRAP 20mM, Ristocetin 1.5mg/L

P3: ADP 10 mM, COL 2.5mg/mL, AA 0.8mM, TRAP 25mM, Ristocetin 1.5mg/L

P4: ADP 10 mM, COL 1.2mg/mL, AA 1mM, TRAP 10 mM, Ristocetin 1.5mg/L

P5: ADP10 mM, COL 2.5mg/mL, TRAP 10 mM, Ristocetin 1.5 mg/L

Supplemental Table 2

Antibody or other reagent	Source	Identifier	Working Dilution
CD41a - APC	BD Biosciences	#559777 / HIP8	1:100 (flow cytometry)
CD42a - PE	BD Biosciences	#558819 / ALMA.16	1:100 (flow cytometry)
Oct3/4 - PerCP-Cy™5.5	BD Biosciences	#560794 / 40/Oct-3	1:100 (flow cytometry)
Sox2 - Alexa Fluor® 647	BD Biosciences	#560302 / 245610	1:100 (flow cytometry)
Nanog - PE	BD Biosciences	#560483 / N31-355	1:100 (flow cytometry)
IgM - APC	BD Biosciences	#555585 / G155 - 228	1:100 (flow cytometry)
IgG1 - PE	BD Biosciences	#555749 / MOPC-21	1:100 (flow cytometry)
IgG1 - PerCP-Cy™5.5	BD Biosciences	#552834 / MOPC-21	1:100 (flow cytometry)
IgG2a - Alexa Fluor® 647	BD Biosciences	#565365 / MOPC-21	1:100 (flow cytometry)
b-Tubulin	Sigma	#T8328 / AA2	1:200 (IF)
Phalloidin-FITC	Sigma	#P5282	1:400 (IF)
Phalloidin-Atto633	Sigma	#68825	1:400 (IF)
Actin	Sigma	#A5441 / AC-15	1:1000 (WB)
GAPDH	Santa Cruz Biotechnology	sc-32233	1:1000 (WB)
HSC70 (mAb, Clone: 6E1)	Active Motif	#61207	1:1000 (WB)
IgG anti-rabbit H+L Alexa Fluor 633	Thermo Fisher Scientific	#A-21071	1:400 (IF)
IgG anti-mouse H+L Alexa Fluor 546	Thermo Fisher Scientific	#A-11003	1:400 (IF)
IgG anti-rabbit HRP-linked	Cell Signaling Technology	#7074	1:2000 (WB)
IgG anti-mouse HRP-linked	Cell Signaling Technology	#7076	1:2000 (WB)
Src	Abcam	Ab109381	1 :10000 (WB)
Src (Y419)	Abcam	Ab185617	1 :5000 (WB)
Stat3	Cell Signaling Technology	#9132	1 :1000 (WB)
Stat3 (Tyr705) D3A7	Cell Signaling Technology	#9145	1:2000 (WB)
GPIBa (CD42b (MM2/174))	Santa Cruz Biotechnology	Sc80728	1 :500 (WB), 1 :200 (IF)
GPIBa (CD42b SZ2)	Sant Cruz Biotechnology	Sc-59052	1 :500-1:1000 (WB); 0.5 or 1 µg (VWF binding tests), 2 µg (IP)
GPV (CD42d G-11)	Sant Cruz Biotechnology	Sc-271662	1 :500 (WB)
GPIX (CD42a A-9)	Sant Cruz Biotechnology	Sc-166420	1 :500 (WB)
CD61	Beckman Coulter	#IM0540	1 :100 (IF)
PAC-1-FITC	Biolegend	A86877	1 :50 (Flow cytometry)
FLNA (C-TERM)	Abcam	#ab51217	1:200 (IF) – 1:1000 (WB)
VWF	Dako	A0082	1 :1000 (flow cytometry)
Fibrinogen Alexa Fluor 488	Invitrogen™	F13191	1 :200 (flow cytometry)
MLC-2 (Ser19)	Cell Signaling	#3671	1 :100 (IF), 1 :1000 (WB)
MLC-2	Cell Signaling	#3672	1 :1000 (WB)

Supplemental table 2: List of antibodies used, including source, identifier and working dilution

Supplemental Table 3

Reagent	Source	Identifier
hBMP4	Peprotech	#AF-120-05ET
hVEGF	Peprotech	#100-20
hFGF-basic	Peprotech	#100-18B
hIL-6	Peprotech	#200-06
hTPO	Kirin Brewery, Tokyo, Japan	/
hFLT3-L	Celldex Therapeutics, Inc., Needham, USA	/
hSCF	Biovitrum AB, Stockolm, Sweden	/
hEPO	Peprotech	#100-64
hG-CSF	Peprotech	#300-23
hGM-CSF	Peprotech	#300-03
hIL-3	Peprotech	#200-03
CHiR 99021 trihydrochloride	TOCRIS	#4953
Y-27632 dihydrochloride	TOCRIS	#1254
VTN-N	Gibco/Thermo Fisher Scientific	#A14700
Geltrex	Gibco/Thermo Fisher Scientific	#A1413202
StemMACS™ iPS-Brew XF, human	Miltenyi Biotec	130-104-368
StemPro®-34 SFM	Gibco/Thermo Fisher Scientific	#10639011
CytoTune™-iPS 2.0 Sendai Reprogramming Kit	Invitrogen/Thermo Fisher Scientific	#A16517
1-thioglycerol	Sigma	#M6145
Fibrinogen	Sigma	#F8630
Fitronectin	Gibco™/ Thermo Fisher Scientific	33016015
Dasatinib	Sigma	CDS023389
Hoechst 33342	Sigma	14533
Nocodazole	Sigma	M1404
Ristocetin	Clinisciences	C4176
von Willebrand Factor (WILFACTIN)	LFB	/

Supplemental table 3: List of reagents used, including source and identifier

Supplemental Figure 1

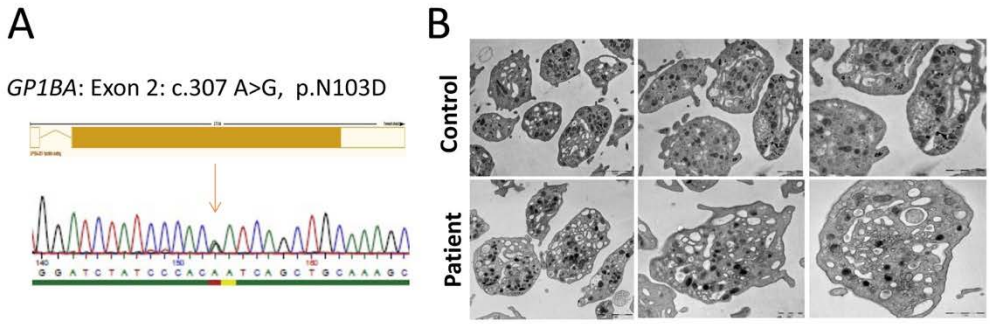

Supplemental Figure 1. Characterization of the patient's blood platelets and *GP1BA* gene mutation. A. Sanger sequencing confirming the heterozygous c.307A>G substitution in *GP1BA* leading to a p.Asn103Asp (p.N103D) change within LRR4 of GPIbα. **B.** Transmission electron microscopy (TEM) of the patient's and control platelets. For the patient, platelets are of increased size.

Supplemental Figure 2

A

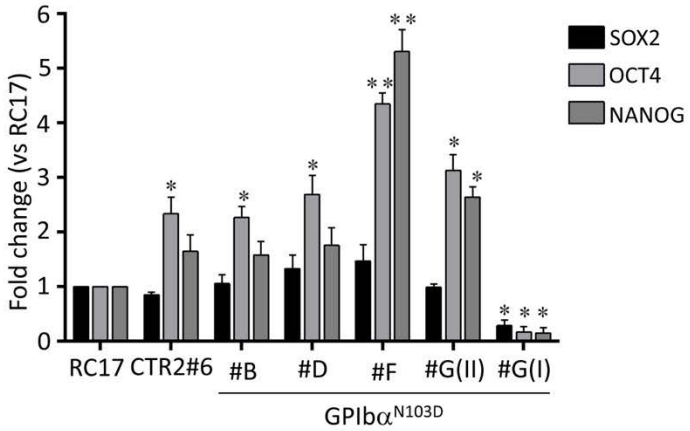

B

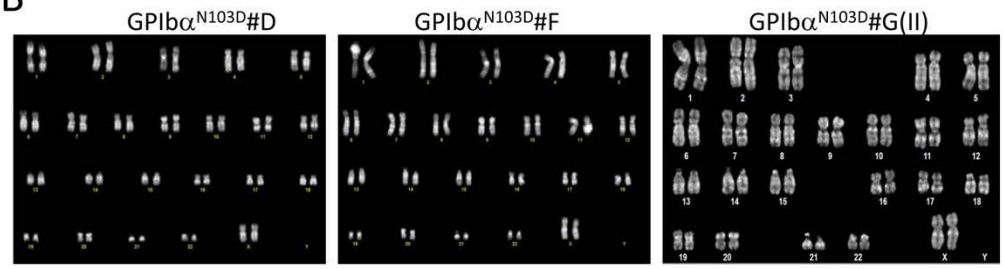

C

Locus Repeat	#STR Genotype		
	GPIBα^{N103D}#D	GPIBα^{N103D}#F	GPIBα^{N103D}#G(II)
TH01	7, 8	7, 8	7, 8
D21S11	31.2, 32.2	31.2, 32.2	31.2, 32.2
D5S818	12, 12	12, 12	12, 12
D13S317	12, 13	12, 13	12, 13
D7S820	12, 12	12, 12	12, 12
D16S539	11, 11	11, 11	11, 11
CSF1PO	11, 12	11, 12	11, 12
AMEL	X, X	X, X	X, X
vWA	17, 17	17, 17	17, 17
TPOX	8, 11	8, 11	8, 11

Supplemental Figure 2. Characterization of GPIbα iPSC clones B, D, F, GI, GII. A. qRT-PCR analysis of *SOX2*, *OCT4* and *NANOG* transcripts relative to *GAPDH* housekeeping gene and normalized to control line hESCs RC17 cell line. Clone GI expressed lower levels of pluripotency markers than control cell line and was not used for further experiments. **B.** Karyotype analysis showing normal 46, XX karyotype for D, F, GII GPIba iPSC clones. Clone B revealed karyotypic anomalies (not shown) and was not used for further experiments. 32 to 38 total metaphases were analyzed and 13-15 total metaphases were karyotyped by Q-binding method with resolution of 350 bands. **C.** Short Tandem Repeat (STR) Testing Report.

Supplemental Figure 3

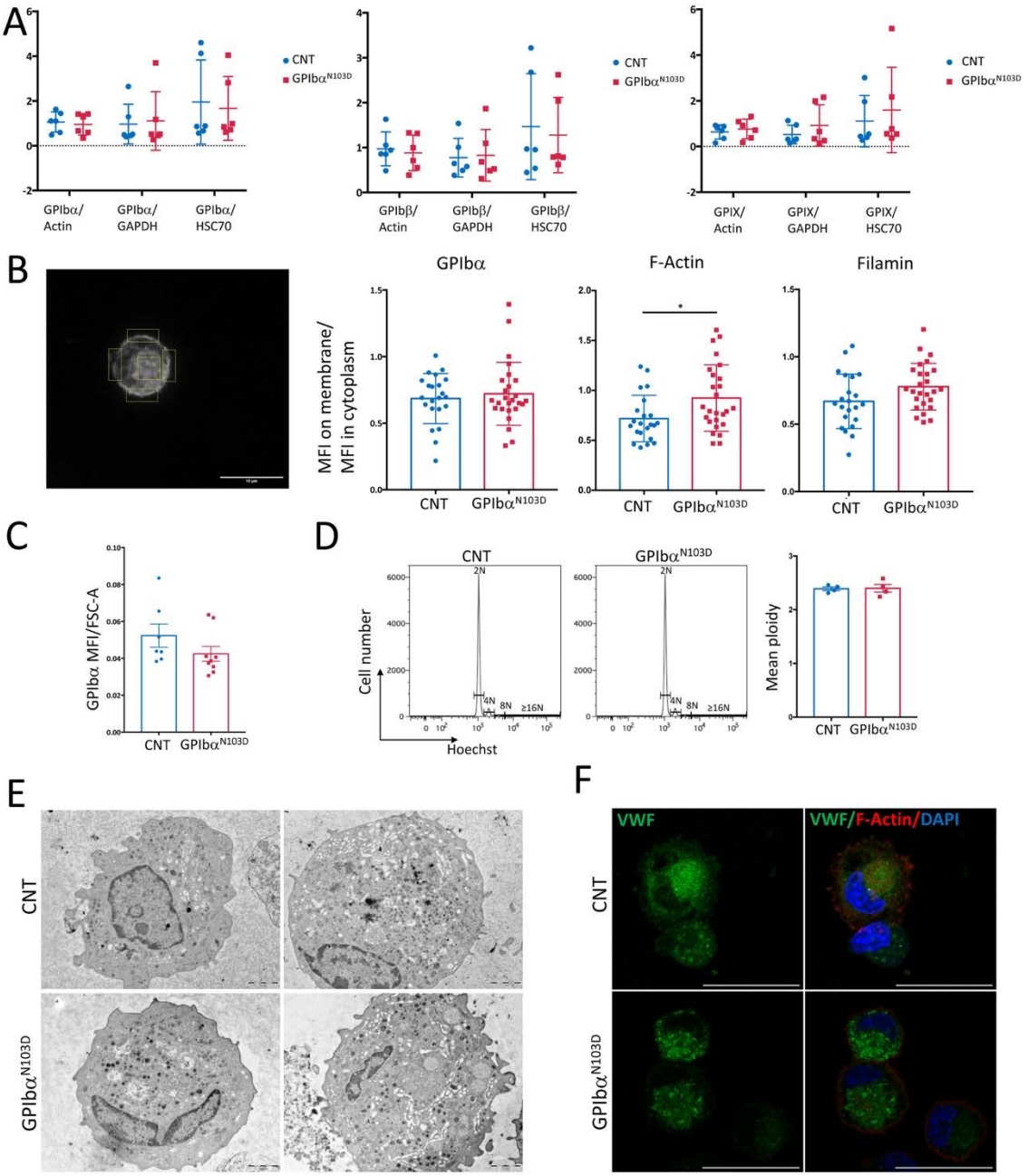

Supplemental Figure 3. GPIbα^{N103D} mutant does not affect the expression of GPIb/GPIX complex and megakaryocyte differentiation from iPSC. A. Western blot analysis and quantification of GPIbα, GPIbβ and GPIX relative to three houskeeping proteins, Actin, GAPDH and HSC70. The histograms show quantification of the WBs representing averages of 3 independent experiments performed each on two independent CNT and GPIbα^{N103D} clones as mean±SD, unpaired t-test. **B.** Fluorescence analysis of CD42b (GPIbα); F-Actin and Filamin distribution in MKs. On the left: a representative picture of MK with rectangles and square depicting the areas of fluorescence measurement, z-stack middle frame is shown. On the right: the histograms presenting the quantification of GPIbα, F-Actin and Filamin. The ratio between Mean Fluorescence Intensity (MFI) measured on membrane and MFI measured in the center of cell is shown as mean±SD, *P<0.05, unpaired t-test. At least 11 MKs were analyzed for each

of two controls (CNT) and two GPIbα^{N103D} clones. **C.** Quantification of GPIbα expression on MKs by flow cytometry. The GPIbα MFI was divided by FSC_A to normalize by MK size. The results of five independent experiments performed on two different CNT and GPIbα^{N103D} clones are shown as mean±SEM, Mann-Whitney test. **D.** Ploidy analysis of control (CNT) and GPIbα^{N103D} (CD41^{+}CD42^{+}) MKs. On the left: representative picture of flow cytometry analysis. On the right: the histograms showing mean ploidy as mean±SEM, unpaired t-test, n=4. **E.** Representative transmission electron microscopy pictures of mature control (CNT) an GPIbα^{N103D} MKs (scale bar: 2 μm). **F.** Representative immunofluorescence staining pictures of mature control (CNT) an GPIbα^{N103D} MKs: F-Actin (red), VWF (green), DAPI (nuclei, blue). Scale bar: 10 μm, z-stack middle frame is shown.

Supplemental Figure 4

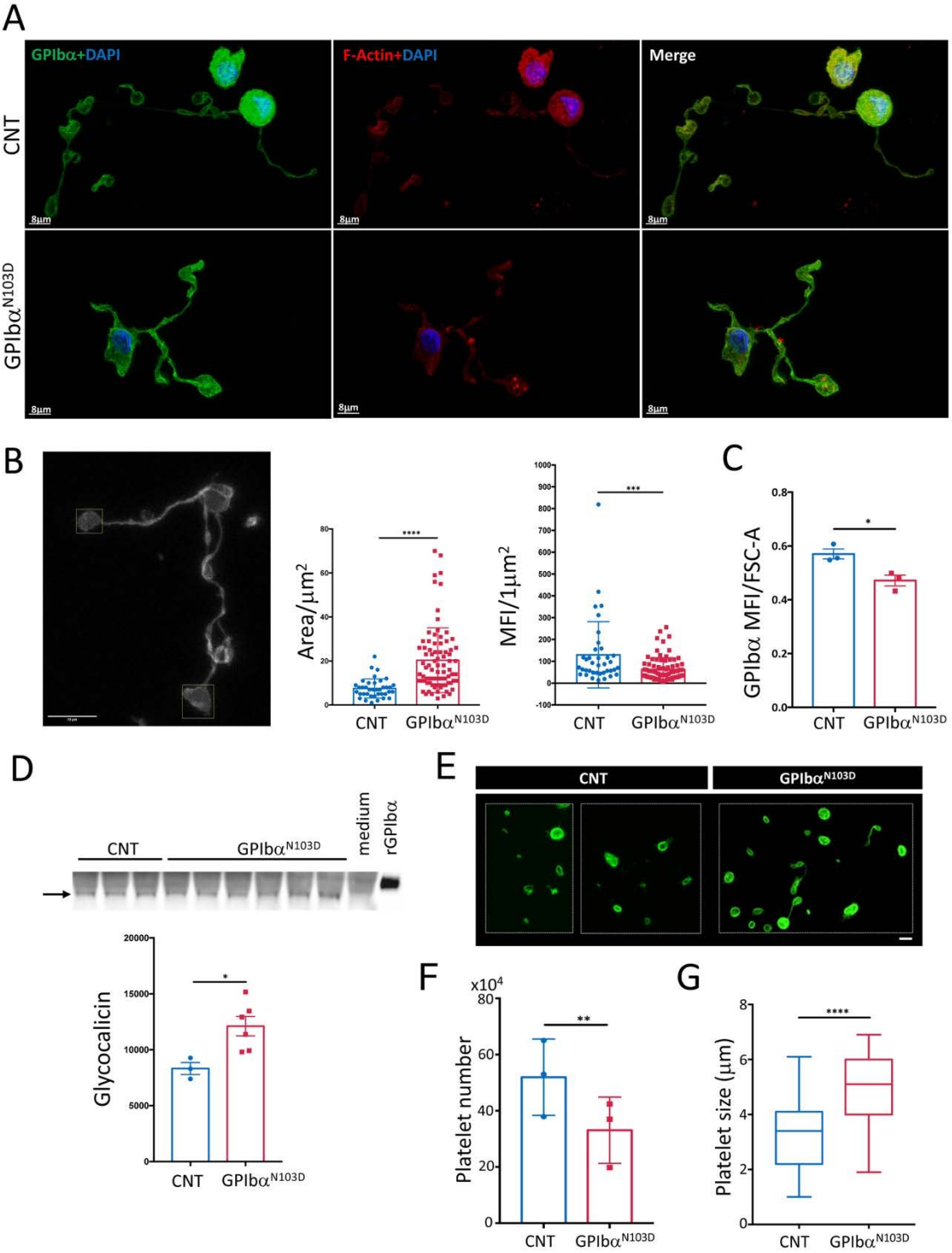

Supplemental Figure 4. GPIbα^{N103D} proplatelets display a slightly decreased GPIbα expression on tips as compared to controls. A. Representative immunofluorescence staining pictures of control (CNT) an GPIbα^{N103D} proplatelet forming MKs: CD42b (GPIbα, green), F-Actin (red), DAPI (nuclei, blue). Scale bar: 8µm, maximal projection is shown. **B.** Quantification of GPIbα expression. On the left: a representative picture of proplatelet forming-MK with squares depicting the areas of fluorescence measurement, z-stack middle frame is shown. On the right: the histograms presenting area (µm^2), and the Mean Fluorescence Intensity (MFI) of GPIbα, reported per 1µm2 as mean±SD, ***P<0.0005, unpaired t-test. At least 16

tips were analyzed for each of two control (CNT) and two GPIbα^{N103D} clones. **C.** Quantification of GPIbα expression on platelet-like particles generated *in vitro* by flow cytometry. The GPIbα MFI was divided by FSC_A to normalize by platelet size. The results of three independent experiments performed on three different CNT and GPIbα^{N103D} clones are shown as mean±SEM, **P*<0.01, Mann-Whitney test. **D.** Quantification of glycocalicin in culture media. Western blot analysis of glycocalicin in culture supernatants, rGPIb was used as a positive control[2] (increased size is due to a Tag) and medium without cells as negative control. The quantity of glycocalicin is expressed in arbitrary units as mean ± SEM (CNT: n=3, GPIbα^{N103D} n=6), **P*<0.05, unpaired t-test. **E-G.** Platelets recovered from the 3D silk bone marrow model functionalized with fibronectin (50 µg/mL). **E.** Representative picture of *ex vivo*-released control (CNT) and GPIbα^{N103D} platelets stained for β-tubulin (green). Scale bar: 5 µm, maximal projection is shown. **F.** The number of recovered platelets, data are expressed as mean ± SEM (CNT n=3, GPIba^{N103D} n=3), ***P*<0.01, unpaired t-test. **G.** Platelet diameters (µm) of *ex vivo*-released platelets measured by Arivis Vision 4D (Zeiss). Data are expressed as mean ± min to max, CNT: n=75, GPIbα^{N103D}: n=75, **P*<0.05, unpaired t-test.

Supplemental Figure 5

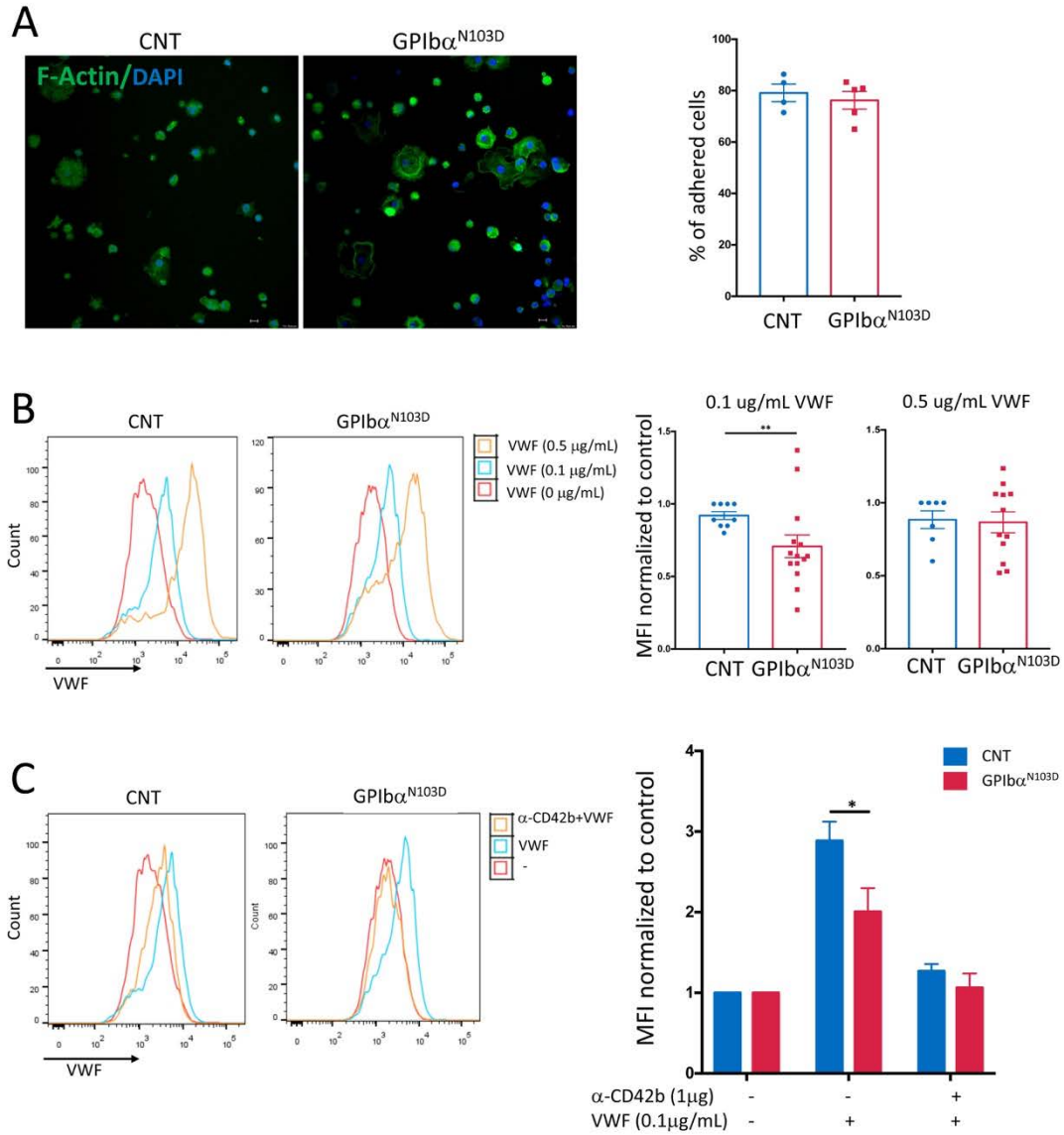

Supplemental Figure 5. Decreased VWF binding to GPIbα^{N103D} mutant. A. Mature control (CNT) and GPIbα^{N103D} Mks were adhered for 30 min on slides coated with 1µg/mL of VWF. Representative pictures of immunofluorescence staining of F-Actin (green) and DAPI (nuclei, blue) are shown on the left, single z-stack frame at the glass adhesion site is shown. The histogram on the right represents the percentage of adhered cell. Data are expressed as mean ± SEM (CNT n=4, GPIbα^{N103D} n=5). **B.** Flow cytometry analysis of ristocetin-induced VWF binding to mature control (CNT) and GPIbα^{N103D} MKs. Representative plots are shown on the left panel. Different concentrations of VWF were used as indicated. Mean fluorescence was normalized to one control (CNT) cell line in each experiment (on the right panel). Four independent experiments were done with at least two different CNT lines and three different GPIbα^{N103D} clones in each experiment. Data are expressed as mean ± SEM (CNT n=9, GPIbα^{N103D} n=14), $^{**}P<0.01$, Mann-Whitney test **C.** Representative pictures of flow cytometry plots showing the VWF binding on mature control (CNT) and GPIba^{N103D} MKs incubated with 1 ug of human anti-CD42b monoclonal antibody prior to incubation with ristocetin- and 0.1 µg/mL of VWF. Mean fluorescence intensity (MFI) was normalized to control cell lines (on the right panel). Data are expressed as mean ± SEM (CNT n=3-5, GPIbα^{N103D} n=3), $^{*}P<0.05$ unpaired t-test.

Supplemental Figure 6

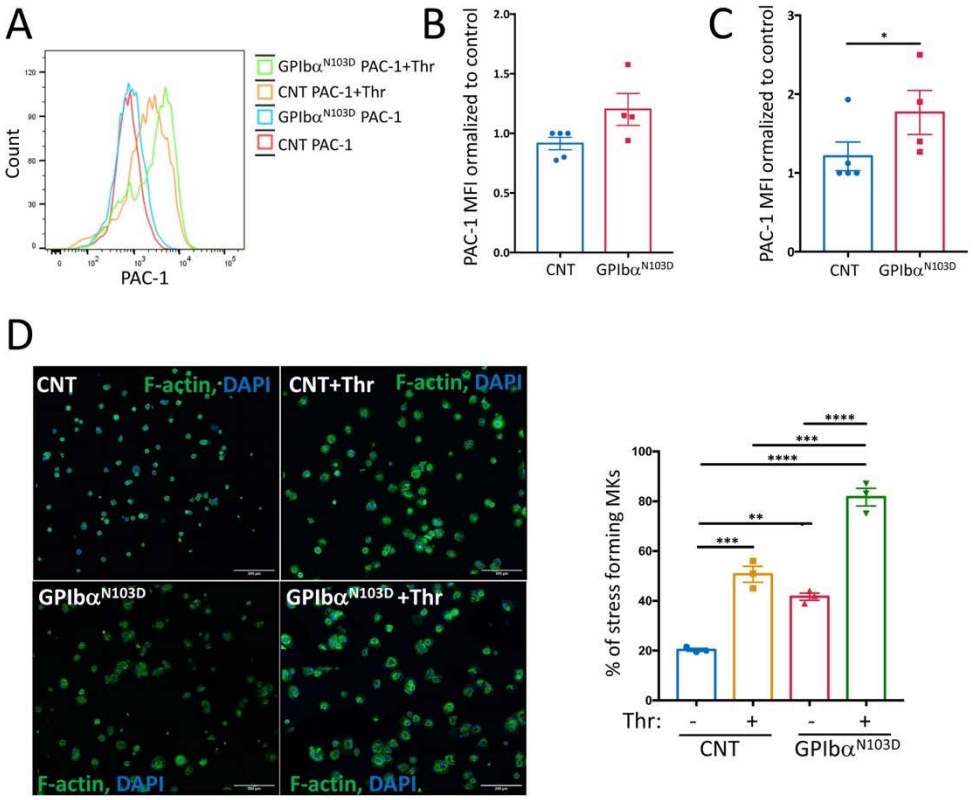

Supplemental Figure 6. Analysis of αIIbβ3 receptor activation. Flow cytometry analysis of PAC-1 binding to αIIbβ3 receptor on control (CNT) and GPIbα^{N103D} mutant MKs at basal state and after its activation by Thrombin (Thr). Monoclonal PAC-1-APC antibody that recognizes the fibrinogen binding site exposed on the activated form of the αIIbβ3 receptor was used. **A.** Representative picture of plots is shown on the left panel. **B-C.** The histograms present the mean fluorescence intensity (MFI) of PAC-1 normalized to 1 control in each experiment. Three independent experiments are shown. Data are expressed as mean ± SEM (CNT n=5, GPIba^{N103D} n=4). **P*<0.05, Mann-Whitney test. **B.** Basal state. **C.** MKs were stimulated for 5 minutes with Thrombin (1U/mL). **D.** Immunofluorescence analysis of stress fibers formation by mature control (CNT) and GPIbα^{N103D} mutant MKs stimulated with thrombin (Thr). Mature MKs were plated on fibrinogen-coated surface in the presence or absence of thrombin (1U/mL) for 30 min and stained for F-Actin (green) and DAPI (blue). Representative pictures of immunofluorescence staining are shown on the left panel. Scale bar: 200 µm, single z-stack frame at the glass adhesion site is shown. The histogram presenting the frequency (%) of stress fiber forming MKs plated on fibrinogen-coated surface in the presence or absence of thrombin is on the right panel. Data are expressed as mean ± SEM, n=4, ***P*<0.01, ****P*<0.005, *****P*<0.001. One Way Analysis of Variance (ANOVA) with Tukey's multiple comparison method was used.

Supplemental Figure 7

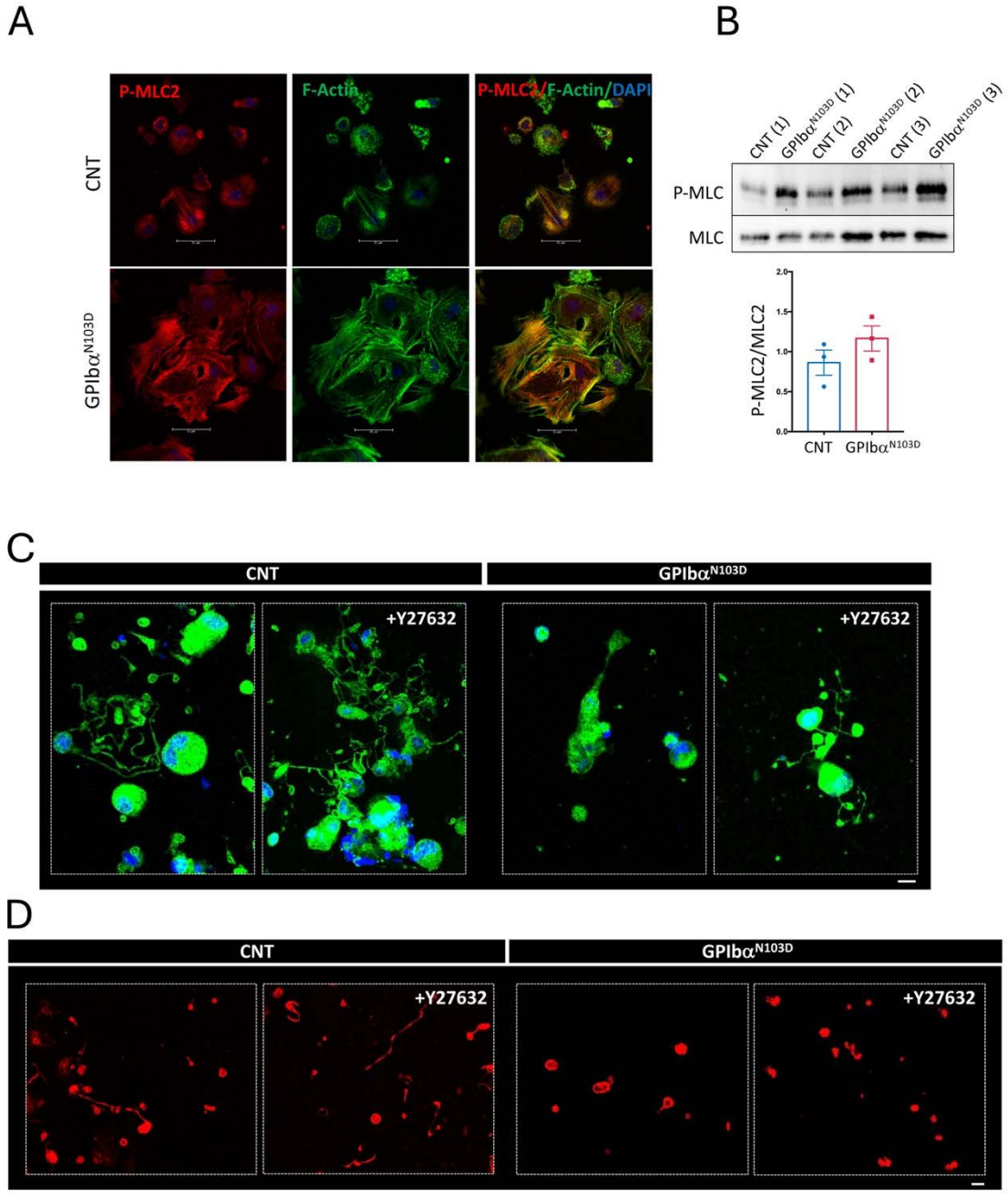

Supplemental Figure 7. GPIbα^{N103D} induces RhoA activation in megakaryocytes. A. Representative pictures of P-MLC2 (red), F-Actin (green) and DAPI (blue) staining of control (CNT) and GPIbα^{N103D} mutant MKs after adhesion on Fibrinogen, single z-stack frame at the glass adhesion site is shown. **B.** Western blot analysis of P-MLC2 in control (CNT) and GPIbα^{N103D} mutant MKs after 30 min incubation on fibrinogen-coated surface. Immunoblots were probed with Abs directed against P-MLC2, and MLC-2. Picture of immunoblot is shown on the top panel. Quantification of P-MLC2/total MLC2 is shown on the bottom panel. Data are expressed as mean±SEM, n=3. **C.** Immunofluorescence analysis of proplatelet formation by mature control (CNT) and GPIbα^{N103D} mutant MKs. Mature MKs were adhered on the fibrinogen-coated surface in the presence or absence of ROCK1/2 inhibitor Y27632, for 24 hours and stained for β-tubulin (green) and DAPI (blue). Scale bar: 10 µm, maximal projection is shown. **D.** Representative picture of *ex vivo*-released platelets with or without ROCK1/2 inhibitor Y27632 stained for β-tubulin (red). Scale bar: 5 µm, maximal projection is shown.

Supplemental Figure 8

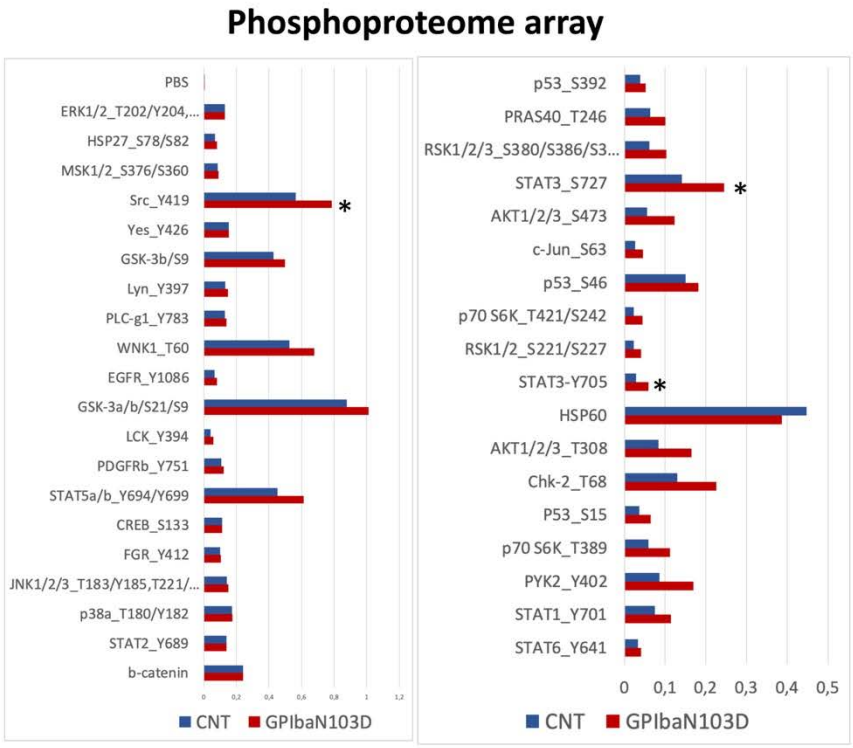

Supplemental Figure 8. Phosphoproteome analysis of control (CNT) and GPIbα^{N103D} mutant MKs. Mature MKs were seeded on fibrinogen-coated surface for 30 min, lysed and phospho-kinases were analyzed using membrane-based human phospho-kinase antibody array. The second experiment is shown.

Supplemental Figure 9

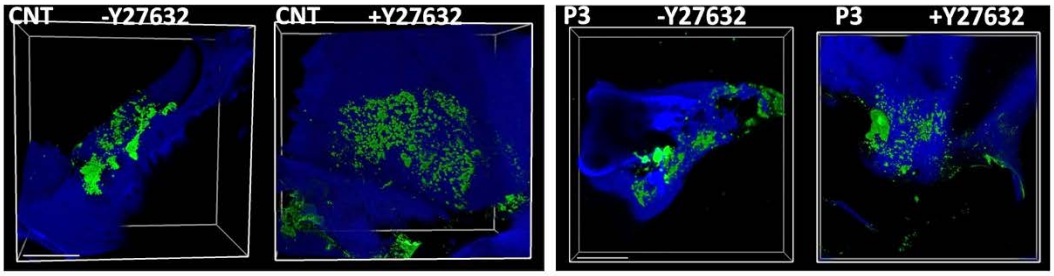

Supplemental Figure 9. RhoA inhibition restores platelet production from GPIbα^{N103D} megakaryocytes. MKs were seeded into the silk sponge with or without ROCK1/2 inhibitor Y27632. Representative picture of control and P3 proplatelet forming MKs. MKs and platelets are stained with anti-CD61 antibody (green) and silk sponge is in blue. Scale bar: 50 μm, full 3D volume is shown.

Supplemental Figure 10

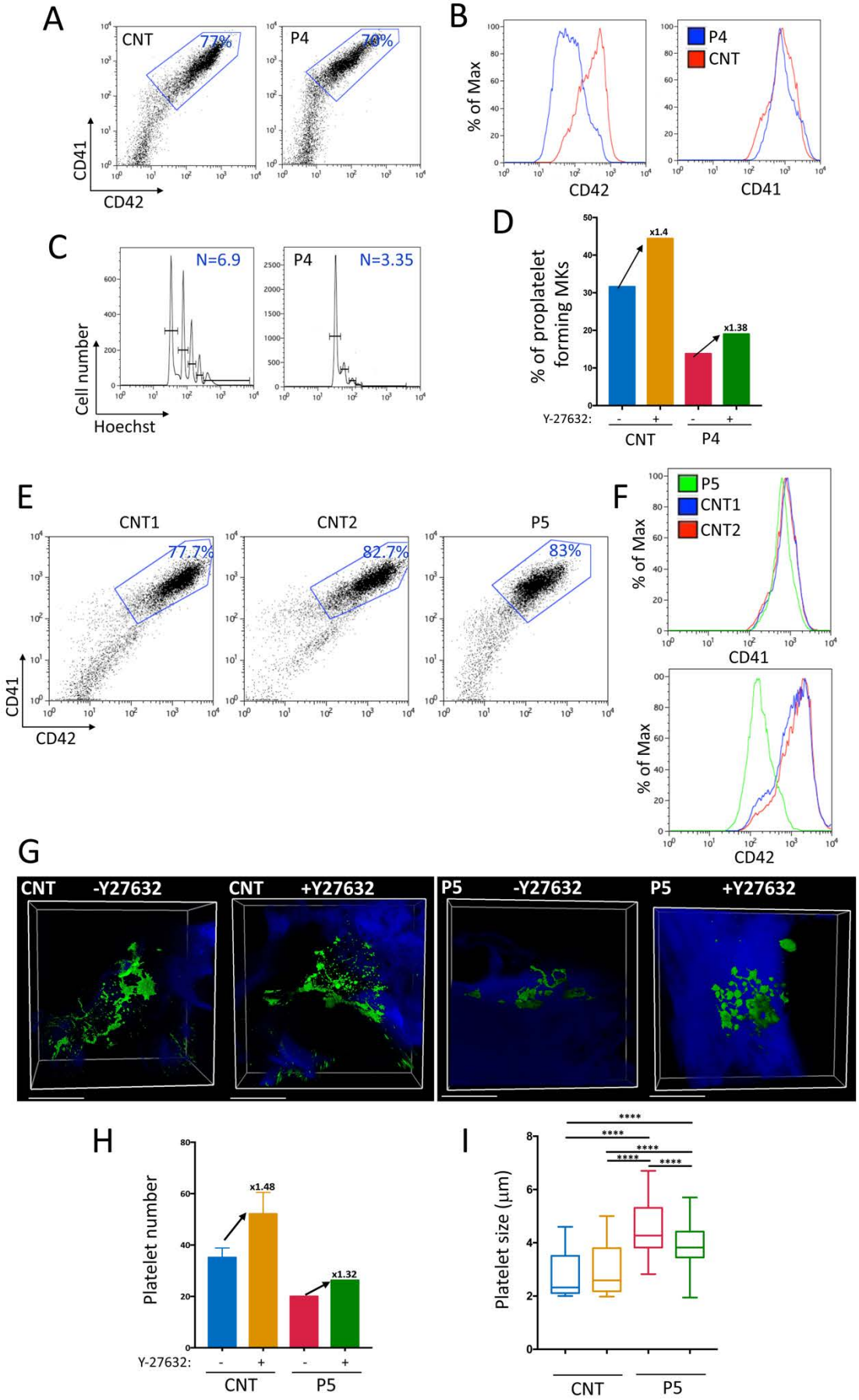

Supplemental Figure 10. RhoA inhibition does not affect platelet generation in homozygous BSS. Hematopoietic progenitors were isolated from peripheral blood of three healthy controls and two patients carrying homozygous *GP1BB* p.G43W (P4) and *GP1BA* p.L139P (P5) mutation respectively and cultured in presence of TPO and SCF for 10 days. **A-C.** Flow cytometry analysis of control (CNT) and patient 4 (P4) MKs. **A.** % of mature $CD41^+CD42^+$ MKs. **B.** CD41 and CD42 expression level. **C.** Ploidy level. $CD41^+CD42^+$ cells were incubated with Hoechst for 2h to label nucleus. N represents a mean ploidy level. **D.** Mature MKs were cultured on fibrinogen-coated surface in presence or absence of ROCK1/2 inhibitor Y27632 for 3 days. The histogram represents the frequency (%) of proplatelet forming MKs. A 1.4-fold increase was detected for control after incubation with ROCK1/2 inhibitor and 1.38-fold increase for P4 after incubation with ROCK1/2 inhibitor. **E-F.** Flow cytometry analysis of two control (CNT1, CNT2) and patient 5 (P5) MKs. **E.** % of mature $CD41^+CD42^+$ MKs. **F.** CD41 and CD42 expression level. **G-I.** MKs were seeded into the silk sponge with or without ROCK1/2 inhibitor Y27632. **G.** Representative picture of control and P5 proplatelet forming MKs. MKs and platelets are stained with anti-CD61 antibody (green) and silk sponge is in blue. Scale bar: 50 μm, maximal projection is shown. **H.** Silk scaffolds were perfused with culture media for 6 hours, and released platelets were collected into gas-permeable bags. Samples were mixed with counting beads to quantify the number of platelets that are identified as $CD41^+CD42a^+$ events. The number of recovered platelets is normalized to control (CNT). A 1.48-fold increase in platelet number was detected for controls after incubation with ROCK1/2 inhibitor (n=3, data are presented as mean±SD) and 1.32-fold increase for P5 after incubation with ROCK1/2 inhibitor. **I.** Platelet diameters (μm) of *ex vivo*-released platelets with or without ROCK1/2 inhibitor Y27632 were measured by Arivis Vision 4D (Zeiss). Data are expressed as mean ± min to max, CNT: n=83, CNT+Y27632: n=83, P3: n=83, P3+Y27632: n=89, ****P<0.0001, One Way Analysis of Variance (ANOVA) with Tukey's multiple comparison method was used.

Supplemental References

1. Latger-Cannard V, Philippe C, Bouquet A, et al. Haematological spectrum and genotype-phenotype correlations in nine unrelated families with RUNX1 mutations from the French network on inherited platelet disorders. *Orphanet J Rare Dis*. 2016;11:49.
2. Vanhoorelbeke K, Cauwenberghs N, Vauterin S, et al. A reliable and reproducible ELISA method to measure ristocetin cofactor activity of von Willebrand factor. *Thromb Haemost.* 2000;83(1):107-113.
3. Otsu, N. A threshold selection method from gray-level images. *IEEE Transactions on Systems, Man, and Cybernetics.* 1979; 9(1), 62-66.
4. Rockwood DN, Preda RC, Yücel T, Wang X, Lovett ML, Kaplan DL. Materials fabrication from Bombyx mori silk fibroin. *Nat Protoc*. 2011;6(10):1612-1631.
5. Di Buduo CA, Soprano PM, Tozzi L, et al. Modular flow chamber for engineering bone marrow architecture and function. *Biomaterials*. 2017;146:60-71.
6. Di Buduo CA, Laurent PA, Zaninetti C, et al. Miniaturized 3D bone marrow tissue model to assess response to Thrombopoietin-receptor agonists in patients. *Elife*. 2021;10.
7. Di Buduo CA, Wray LS, Tozzi L, et al. Programmable 3D silk bone marrow niche for platelet generation ex vivo and modeling of megakaryopoiesis pathologies. *Blood*. 2015;125(14):2254-2264.
8. Donada A, Balayn N, Sliwa D, et al. Disrupted filamin A/α(IIb)β(3) interaction induces macrothrombocytopenia by increasing RhoA activity. *Blood*. 2019;133(16):1778-1788.